Increase in Ion Temperature by Slow Wave Heating in Magnetosphere Plasma Device RT-1[*]

Masaki NISHIURA, Zensho YOSHIDA, Yoshihisa YANO, Yohei KAWAZURA,
Toshiki MUSHIAKE, Haruhisa SAITOH, Miyuri YAMASAKI, Ankur KASHYAP,
Noriki TAKAHASHI, Masataka NAKATSUKA, Yuichi TAKASE and Atsushi FUKUYAMA[1]

Graduate School of Frontier Sciences, The University of Tokyo, 5-1-5 Kashiwanoha, Kashiwa 277-8561, Japan
[1]Department of Nuclear Engineering, Kyoto University, Nishikyo-ku, Kyoto 615-8540, Japan

Ion cyclotron range of frequencies (ICRF) heating with a frequency of a few MHz and an input power of 10 kW was applied for the first time, to the best of our knowledge, in a magnetosphere plasma device. An antenna was installed near the pole of a dipole field for slow-wave excitation. Further, a ∩-shaped antenna was implemented and characterized for efficient ion heating. Electron cyclotron heating with an input power of 8 kW sustained helium plasmas with a fill gas pressure of 3 mPa. ICRF heating was then superimposed onto the target plasma (H, D, and He). While the ICRF power was turned on, the increase in ion temperatures was observed for low-pressure helium plasmas. However, the temperature increase was not clearly observed for hydrogen and deuterium plasmas. We discuss the experimental results in terms of power absorption based on result calculated with the TASK/WF2 code.

1. Introduction

The magnetosphere plasma device ring trap-1 (RT-1) enables us to study magnetosphere plasma physics as one of the new concepts for nuclear fusion devices [1]. A diversity of plasmas is expected to be realized with RT-1. Some of these plasmas such as inward diffusion and self-organized plasmas have been observed [2–7]. A dipole magnetic field stably and naturally confines plasma in a high beta state like magnetosphere plasma of planets. In the RT-1 device, a high electron beta state has been achieved via electron cyclotron heating (ECH) [5]. The recent power increase and optimization of ECH has made it possible to achieve a local electron beta $\beta_{e0} > 1$ [6]. These high-energy electrons exist in plasmas; their energy was verified to be approximately a few tens of keV from the X-ray spectrum.

The increase of ion temperatures and ion beta values in RT-1 gives us access to novel plasma physics as well as other interesting topics concerning the understanding of the nature of the inherent physics [8]. To achieve the high ion beta values, ion cyclotron range of frequencies (ICRF) heating has been implemented. The antenna was located at the inner high field side for slow wave excitation. An excited slow wave propagated in the plasma toward the resonance layer of the lower magnetic field in a beach heating configuration [9,10]. Although beach heating has been

widely used in fusion devices and linear devices [10–13], ion heating has obviously not been promising for a magnetosphere configuration. We consider the reasons that the magnetic curvature of magnetosphere devices (RT-1 and LDX [14]) is opposite to that of linear devices and only the poloidal magnetic field exists. Those magnetic field configurations are different for tokamaks and stellarators. Recently, ICRF heating has used a fast wave from the low field side in tokamak and helical devices for nuclear fusion. Therefore, although this fast-wave heating scenario might be a better method in a magnetosphere plasma, we selected beach heating excited by slow wave, because the density range is close to linear devices.

This paper reports the first successful ICRF heating in a laboratory magnetosphere plasma by slow wave excitation.

2. ECH and ICRF Heating in RT-1

In the magnetosphere plasma device RT-1, the confinement region is located radially outside the levitation coil surface. ECH with a frequency of 8.2 GHz and an energy input of ~ 50 kW produces plasmas with hot electrons and energies in the range of a few tens of keV. The electron density typically reaches 10^{17} - 10^{18} m^{-3} for the peak density profile. In the equatorial plane, the local electron beta value exceeds 1 in RT-1 plasmas when the magnetic field strength is ~ 0.04 T at a radius of 0.5 m. In such a situation, the ions still remain cold with energies of a few tens
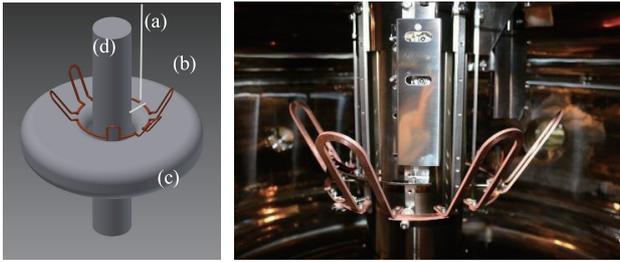
Fig. 1 ∩-shaped antenna in RT-1. (a) Current feedthrough, (b) ∩-shaped antenna, (c) levitation coil, and (d) center stack. The antenna is made of oxide-free copper.
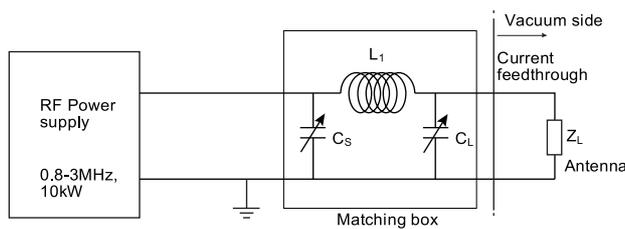
Fig. 2 Schematic of electrical circuit for ICRF heating.

Fig. 3 Ion cyclotron resonance layers, separatrix, and ∩-shaped antenna of RT-1. The field of view useable for spectroscopy measures horizontally in the equatorial plane (Z = 0 m).

of eV because the heating source is dominated by Coulomb collisions between cold electrons and ions. Ion heating is theoretically expected to provide access to high ion beta states and improve the plasma confinement.

The power supply for ICRF heating outputs 10 kW in the frequency range of 0.8 - 3 MHz. A ∩-shaped antenna with six phases was designed to heat ions and electrons, as shown in Fig. 1. The antenna's loop excites a slow wave (ion cyclotron wave) for ion heating by an electric field component $E_\perp$ perpendicular to the magnetic field. The part along the magnetic field excites a parallel electric field component $E_\parallel$ for electron heating. The ∩-shaped antenna is supported at the center stack. One side is connected to the current feedthrough from the power supply and the other side is grounded electrically. Figure 2 shows the electrical circuit for ICRF heating. The capacitance and inductance inside the matching box are adjusted to minimize the reverberating wave in vacuum condition for course tuning during a discharge for fine tuning. The reverberating wave is normally suppressed to below 10% of the forward power during operation.

The ion cyclotron resonance layers and the separatrix of RT-1 are shown in Fig. 3. The ion cyclotron layers for H, D, He, and C are calculated for the frequency f_{rf} = 2 MHz (not shown for H and D). The impurity ion for C^+ has no resonance in this magnetic field range. The levitation coil produces a magnetic field only in the poloidal direction.

RT-1 has two operation modes: supported-coil and levitated-coil modes; in the supported-coil mode, the levitation coil is lifted up by three support rods that are located at $R \sim 0.2$ m from the bottom of the vacuum vessel. This operation mode increases the plasma-loss area by the rods.
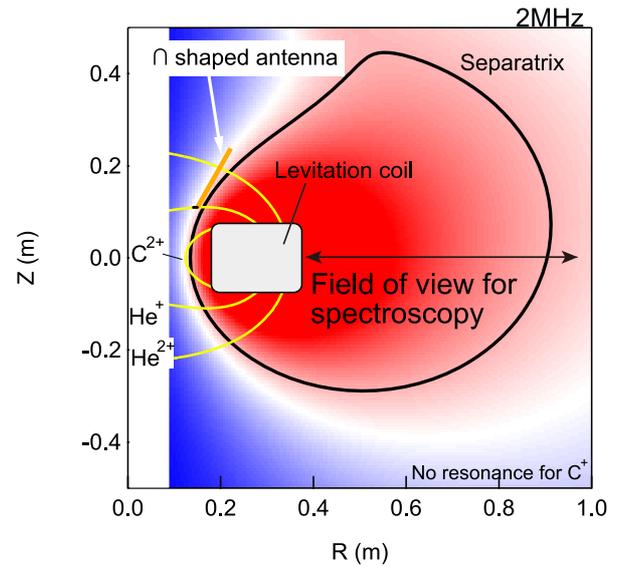
In the levitated-coil mode, the levitation coil is levitated by lifting the magnet from the outside of the vacuum vessel. A target plasma is sustained by 8.2 GHz ECH for 1 s, and ICRF heating is applied with a delay of 0.2 ms after the onset of the ECH injection. Switching ON and OFF of ICRF heating is repeated shot by shot to obtain the radial profiles of the ion temperature distributions. The line of sight for the spectroscopy measures the profiles horizontally in the equatorial plane. Thus, Z is usually located in the Z = 0 plane. The definition of R indicates the radial length that equals the tangency radius because of the toroidal symmetry. We observed a clear increase of the ion temperatures of bulk helium ions (He II, λ = 468.57 nm) and impurity ions (C III, λ = 464.74 nm) in helium plasmas with a gas pressure of 3 mPa if the ICRF power of ∼ 10 kW was comparable to the ECH one, as shown in Fig. 4. In the case of the levitation coil being supported, ion temperature increases for He II and C III were observed at R = 0.4 m. The average temperature of T_i(C III) was increased from 7.6 to 12.7 eV by ICRF heating. The average of T_i(He II) was between 6.3 and 7.3 eV. The ion emission area was localized near the levitation coil surface at R = 0.375 to 0.470 m in the equatorial plane. The emission at larger R was too weak to obtain ion temperatures because three support rods from the bottom side support the levitation coil that increased the loss area.

The relation between diamagnetism and line-integrated electron density at R = 0.45 m is shown in Fig. 5. When the ICRF power was turned on, the electron density decreased and the diamagnetism strength increased. ICRF heating also decreased for the line-averaged densities at R = 0.6 and 0.7 m in the same shot. In this condition, the spatial profiles of ion temperatures
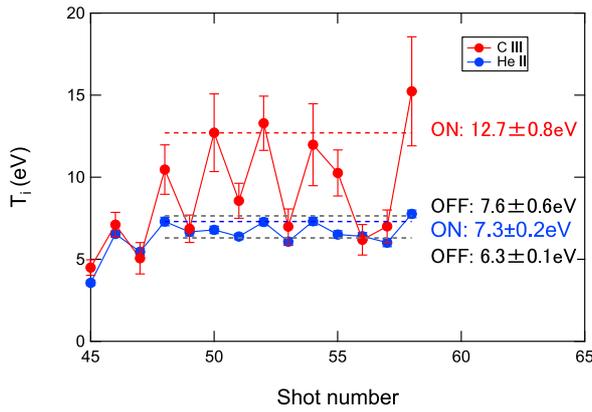
Fig. 4 Ion temperature measured at $R = 0.4\,\mathrm{m}$ for ICRF power with ON and OFF (shots #48 - 58). The levitation coil is supported.
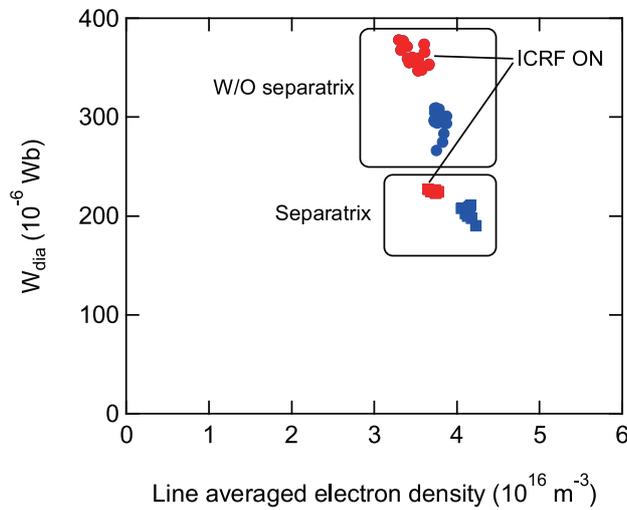
Fig. 5 Relation between diamagnetism and line-averaged electron density during ICRF power ON (red symbols) and OFF (blue symbols). Separatrix (closed squares) and pure dipole (closed circles) configurations are plotted. The levitation coil is supported. $f_{\mathrm{rf}} = 2\,\mathrm{MHz}$.

Fig. 6 Relation between ion temperatures scanned at $R = 0.375 - 0.47\,\mathrm{m}$ and diamagnetism. The levitation coil is supported. $f_{\mathrm{rf}} = 2\,\mathrm{MHz}$.
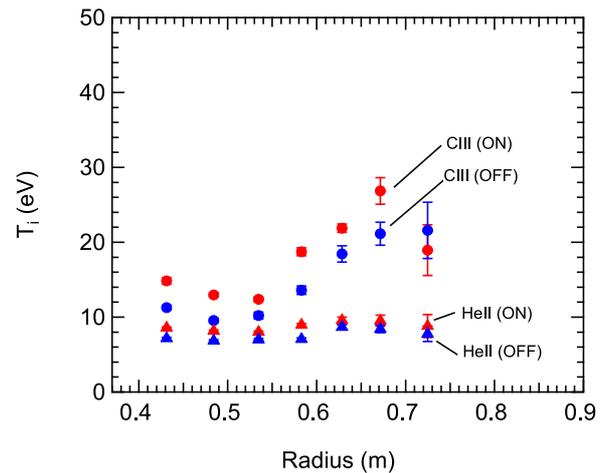
Fig. 7 Spatial profile of T_i during ICRF ON/OFF. The levitation coil is levitated. $f_{\mathrm{rf}} = 2\,\mathrm{MHz}$.

were investigated by spectroscopic measurements. The ion temperatures of He II and C III are plotted in Fig. 6. The magnetic configurations with and without separatrix were varied by the magnetic field of the lifting magnet implemented for the levitation. The measurable area was limited to a small region with R between 0.375 and 0.470 m for this operation condition (the levitation coil was still supported). We found that the ion temperature of He II was relatively low compared with that of C III. The separatrix configuration decreases the ion temperatures as well as the diamagnetism strength.

For the case that the levitation coil was levitated, the ion temperatures of He II and C III were measured (Fig. 7). The difference between ICRF turned on and off was observed to be the same as that for He II and C III. The levitated case extended the measurable area up to $R = 0.73\,\mathrm{m}$.

This was due to the removal of loss area (the support rods were placed at the bottom of the vacuum vessel). The peak of the ion temperature was observed at $R = 0.67\,\mathrm{m}$, and the ion temperature increased uniformly in the measured area.

At an ECH input power of $\sim 10\,\mathrm{kW}$ and a helium gas pressure of 3 mPa, ICRF heating effect was observed as noted above. However, at higher ECH powers and higher gas pressures or with other gases (H and D), ICRF heating effect has not yet been observed. The reason might be a charge exchange loss, as was pointed out for a linear device [13]. It is also important to identify the excited electromagnetic wave as a slow L wave that propagates efficiently in plasmas, as we simulated in the subsequent section.
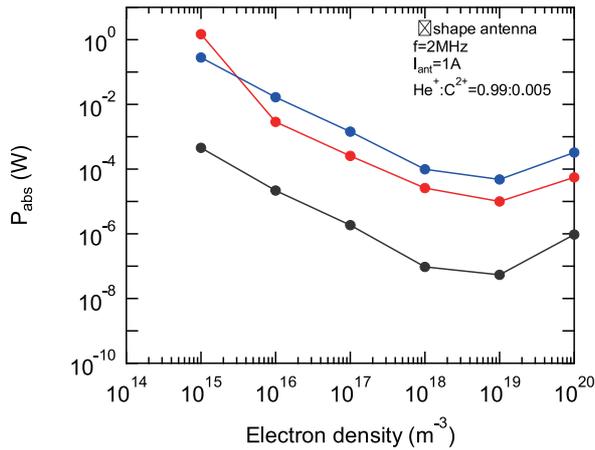
Fig. 8 Dependence of absorption power on electron density (blue: ions, red: electrons, black: C^{2+} impurities).

3. TASK/WF2 Simulation

The propagation and absorption of electromagnetic waves were calculated using the TASK/WF2 code [12]. The poloidal cross section of RT-1 was modeled with a two-dimensional structure. The electron density at the edge was set to be 10^3 times lower than the central electron density, which corresponds to the electron density in Fig. 8. We assumed that the plasma contained the impurity ions C^{2+} of 0.5% and the bulk ions He^+ of 95%. The antenna current was set to 1 A. The simulation results show that the $\cap$-shaped antenna maintains the high absorption power P_{abs} of ions and electrons in the low density region ($\sim 10^{17}$ m^{-3}). This suggests a clear change in T_i for low ECH power operation and leads to ion heating, as described in the previous section. This antenna, however, tends to decrease the absorption power with increasing electron density. The simulated tendency of the absorption power explains the experimental result that high-power ECH operation ($P_{ECH} > P_{ICRF}$) weakens the effect of ICRF heating.

4. Summary

The ICRF heating experiment has been performed in the magnetosphere plasma device RT-1. The effect of ICRF heating was observed for the first time, to our knowledge, in a magnetosphere plasma device; however, the heating effect has not yet been fully understood. We observed the following by implementing a $\cap$-shaped antenna for ICRF heating:

- An increase in T_i was observed due to ICRF heating with 2 MHz and 10 kW of RT-1.

- T_i increased in helium plasma but not in deuterium and hydrogen plasmas, as determined by spectroscopic measurements.
- For the case where P_{ECH} is comparable to P_{ICRF}, an increase of T_i is observed. However, if $P_{ECH} > P_{ICRF}$, the ICRF heating effect is weakened. This tendency is explained by the results of a TASK/WF2 code simulation.

[1] A. Hasegawa, L. Chen and M.E. Mauel, Nucl. Fusion **30**, 2405 (1990).
[2] Z. Yoshida, H. Saitoh, J. Morikawa, Y. Yano, S. Watanabe and Y. Ogawa, Phys. Rev. Lett. **104**, 235004 (2010).
[3] H. Saitoh, Z. Yoshida, J. Morikawa, Y. Yano, T. Mizushima, Y. Ogawa, M. Furukawa, Y. Kawai, K. Harima, Y. Kawazura, Y. Kaneko, K. Tadachi, S. Emoto, M. Kobayashi, T. Sugiura and G. Vogel, Nucl. Fusion **51**, 063034 (2011).
[4] Z. Yoshida, H. Saitoh, Y. Yano, H. Mikami, N. Kasaoka, W. Sakamoto, J. Morikawa, M. Furukawa and S.M. Mahajan, Plasma Phys. Control. Fusion **55**, 014018 (2013).
[5] H. Saitoh, Y. Yano, Z. Yoshida, M. Nishiura, J. Morikawa, Y. Kawazura, T. Nogami and M. Yamasaki, Phys. Plasmas **21**, 082511 (2014).
[6] M. Nishiura, Z. Yoshida, H. Saitoh, Y. Yano, Y. Kawazura, T. Nogami, M. Yamasaki, T. Mushiake and A. Kashyap, Nucl. Fusion **55**, 053019 (2015).
[7] Y. Kawazura, Z. Yoshida, M. Nishiura, H. Saitoh, Y. Yano, T. Nogami, N. Sato, M. Yamasaki, A. Kashyap and T. Mushiake, Phys. Plasmas **22**, 112503 (2015).
[8] Z. Yoshida, S.M. Mahajan, T. Mizushima, Y. Yano, H. Saitoh and J. Morikawa, Phys. Plasmas **17**, 112507 (2010).
[9] T.H. Stix, *Waves in Plasmas* (American Institute of Physics, New York, 1992), pp. 342-343.
[10] Y. Yasaka, Plasma Fusion Res. **75**, 1069 (1999).
[11] J.C. Hosea and R.M. Sinclair, Phys. Fluids **13**, 701 (1970).
[12] Y. Yamaguchi, M. Ichimura, T. Ouchi, I. Kozawa, H. Muro, S. Sato, A. Fukuyama, H. Hojo, M. Katano, Y. Motegi, J. Ohishi, T. Murakami, Y. Sekihara and T. Imai, Trans. Fusion Sci. Technol. **55**, 106 (2009).
[13] M. Inutake, A. Ando, K. Hattori, H. Tobari, T. Makita, M. Shibata, Y. Kasashima and T. Komagome, Plasma Phys. Control. Fusion **49**, A121 (2007).
[14] A.C. Boxer, R. Bergmann, J.L. Ellsworth, D.T. Garnier, J. Kesner, M.E. Mauel and P. Woskov, Nature Physics **6**, 207 (2010).